Journal of Hazardous Materials 186 (2011) 306–312

Contents lists available at ScienceDirect

Journal of Hazardous Materials

journal homepage: www.elsevier.com/locate/jhazmat

Vancomycin-functionalised Ag@TiO_2 phototoxicity for bacteria

Yi Wan, Dun Zhang*, Yi Wang, Peng Qi, Jiajia Wu, Baorong Hou

Chinese Academy of Sciences, Key Lab of Corrosion Science, Shandong Province, Institute of Oceanology, 7 Nanhai Road, Qingdao 266071, China

ARTICLE INFO

Article history:
Received 20 May 2010
Received in revised form
30 September 2010
Accepted 30 October 2010
Available online 10 November 2010

Keywords:
Phototoxicity
Sulphate-reducing bacteria
Vancomycin
Photocatalyst

ABSTRACT

This study reports on the synthesis of vancomycin (Van)-functionalised Ag@TiO_2 nanoparticles and their enhanced bactericidal activities. Van-Ag@TiO_2 nanoparticles were prepared by nanoparticle deposition and chemical cross-linking reactions. The catalysts showed high efficiency for the degradation of methylene blue under ultraviolet (UV) illumination. The photocatalytic inactivation of the sulphate-reducing bacteria, *Desulfotomaculum*, was also studied under UV light irradiation and in the dark using aqueous mixtures of Ag, Ag@SiO_2, Ag@TiO_2, and Van-Ag@TiO_2. The Van-Ag@TiO_2 nanoparticles showed a capacity to target Van-sensitive bacteria. They also effectively prevented bacterial cell growth through the functionalised nanoparticles under UV irradiation for 1 h. To investigate the specificity of the catalyst phototoxicity, a Van-resistant bacteria, *Vibrio anguillarum*, was used as the negative control. The results indicated that Van-Ag@TiO_2 nanoparticles had a higher selective phototoxicity for Van-sensitive bacteria. Therefore, the antibiotic molecule-functionalised core–shell nanoparticles allow for selective photokilling of pathogenic bacteria.

1. Introduction

Sulphate-reducing bacteria (SRB) are anaerobic microorganisms that use sulphate as a terminal electron acceptor to produce sulphide. The highly corrosive and toxic metabolic product of sulphide poses a serious problem for industries, such as the offshore oil industry, as well as economies and ecological systems. Therefore, a rapid and facile method for monitoring and inhibiting SRB growth is essential for the control of microbiologically induced corrosion and water contamination.

Traditional methods for bacterial inactivation, such as chlorination, ultraviolet (UV) sterilisation, and ozone, effectively inhibit and kill pathogenic bacteria [1,2]. However, conventional bactericidal technology can lead to harmful substances like trihalomethanes, which are known for their high carcinogenic capacity [3]. One promising technology to address this concern is photocatalysis, which is considered an advanced method for solving environmental problems [4,5]. Recently, TiO_2 nanoparticles were introduced as possible photocatalysts in the destruction of bacteria [6,7].

When illuminated by near-UV light, TiO_2 exhibits excellent bactericidal activity. This is because some reactive oxygen species like hydrogen peroxide (H_2O_2), hydroxyl radical ($OH^{\bullet}$), and superoxide ($O_2^{\bullet -}$), which are generated from the photocatalytic process, can damage microorganisms [8]. Metal or metal complex-doped TiO_2 were found to be significantly more photocatalytically and antimicrobially active than uncoated TiO_2 nanoparticles under light [7]. For example, Zhang et al. verified that Ag/TiO_2 synthesised by a triblock copolymer can induce the reduction of Ag ions in ethanol with enhanced photocatalytic and bactericidal activities [8,9]. The catalyst AgBr/TiO_2 was found to be highly photocatalytic in the destruction of bacteria in water under visible light [10]. Hu et al. found that Ag/AgBr/TiO_2 exhibits high photocatalytic activity, not only in the degradation of azodyes but also in the destruction of bacteria under visible light irradiation [11]. The apatite-coated Ag/AgBr/TiO_2 fabricated by Ghoami et al. bears a significantly high photocatalytic activity under light and also possesses a high ability to absorb bacteria, resulting in bacterial inactivation in the dark [12]. Wu et al. further reported a composite photocatalyst of PdO/TiO_2, which significantly inactivated bacteria under visible light [13]. In addition, N and C co-doped TiO_2 enables photocatalytic inactivation of bacteria under visible and UV light [14]. However, these composite nanoparticles that are activated under visible or UV light are capable of killing various microorganisms, not only a specific kind of bacteria.

Vancomycin (Van) is an antibiotic that can be attached to nanoparticles. It is capable of enhancing antimicrobial activities [15] because of its well-established ligand–receptor interaction and the specific recognition of Van-sensitive bacteria [16]. Vancomycin acts by inhibiting cell wall synthesis in bacteria. In this way, the antibiotic molecule is able to form a five-point hydrogen bond that is connected with the terminal D-Ala-D-Ala moieties to prevent the incorporation of the *N*-acetylmuramic acid-peptide and *N*-acetylglucosamine-peptide subunits into the peptidoglycan matrix. This mechanism inhibits bacterial growth. Various

* Corresponding author. Tel.: +86 532 82898960; fax: +86 532 82898960.
E-mail address: zhangdun@ms.qdio.ac.cn (D. Zhang).

0304-3894/$ – see front matter © 2010 Elsevier B.V. All rights reserved.
doi:10.1016/j.jhazmat.2010.10.110

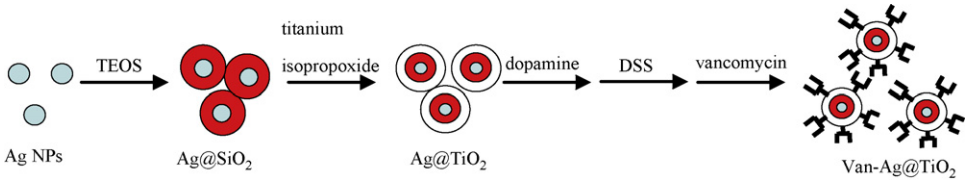

Scheme 1. Steps in fabricating Van-Ag@TiO_2 nanoparticles.

factors are related to the entrance of substances into the outer membrane of Van-resistant organisms, indicating that Van is not active against Van-resistant bacteria. Gu et al. reported the use of Van-biofunctional magnetic nanoparticles to capture Van-resistant enterococci and other Gram-positive bacteria at ultra-low concentrations in a short time [17]. Kell et al. [18] further developed a series of Van-modified nanoparticles to isolate a variety of pathogens from a complicated matrix. They found that only one orientation of Van on the surface of nanoparticles is critical in mediating fast and effective interactions between the functionalised nanoparticles and the cell wall surface of the Gram-positive bacteria.

In this paper, we prepared Van-Ag@TiO_2 based on the nanoparticle deposition and chemical cross-linking reactions. The visible light-driven photocatalytic activity of Van-Ag@TiO_2 nanoparticles was investigated for the decomposition of methylene blue (MB). Van-Ag@TiO_2 nanoparticle visible-light photocatalyst for the destruction of Gram-positive bacteria was characterised by X-ray diffraction (XRD), transmission electron microscopy (TEM), and Fourier transform infrared (FT-IR) spectroscopy.

2. Experimental

2.1. Chemicals and materials

All chemicals used were of the highest purity. Silver nitrate, D-glucose, sodium dodecylsulphate (SDS), ammonia (25%, w/w, aqueous solution), and MB were purchased from Sinopharm Chemical Reagent Co., Ltd. Tetraethyl orthosilicate (TEOS), titanium (IV) isopropoxide, dopamine hydrochloride, suberic acid bis(*N*-hydroxysuccinimide ester) (DSS), and vancomycin hydrochloride were obtained from Sigma–Aldrich. All solvents used were of analytical grade and provided by Sinopharm Chemical Reagent Co., Ltd. The Gram-negative bacterium, *Vibrio anguillarum*, was contributed by Dr. Zhaolan Mo and used in the negative control experiment.

2.2. Synthesis of Van-functionalised TiO_2/Ag nanoparticle

The preparation of Van-functionalised TiO_2/Ag nanoparticles is shown in Scheme 1. In details, silver nitrate (0.51 g) was dissolved in 50 mL of Mili-Q water. Aqueous ammonia (1.00 M) was added dropwise to the $AgNO_3$ solution under vigorous stirring until a colorless solution was obtained. This was followed by the addition of 20 mL glucose (0.10 M), 10 mL SDS (0.20 M), and 15 mL Mili-Q water. Sodium hydroxide solution was used to adjust the pH to ca. 11.5. The reaction was allowed to occur for 10 min. The prepared Ag nanoparticles were used for subsequent experiments without any additional modifications.

The Ag nanoparticles (0.10 g) generated above were rinsed thrice with ethanol and then resuspended in ethanol (20 mL) under sonication for 2 h. Ammonia (2.25 mL), Mili-Q water (2.25 mL), and TEOS (0.50 mL) were added to the suspension. The silica-coated nanoparticles were obtained by vortex mixing for another 5 h, isolated by centrifugation, and rinsed thrice with ethanol. The SiO_2-coated Ag nanoparticles were resuspended in Mili-Q water (20 mL), and the mixture was acidified with HCl (0.5 M, 0.22 mL). A solution containing titanium isopropoxide (0.50 mL) and 2-propanol (4.50 mL) was slowly added to the mixture and stirred for 8 h. The Ag@TiO_2 nanoparticles were rinsed thrice with Mili-Q water.

The Ag@TiO_2 nanoparticles (0.10 g) were dispersed and vortexed for 1 h with dopamine (20 mM, 50 mL) in Mili-Q water. After rinsing with DMF, dopamine-modified nanoparticles and Van were bound with a double cross-linking reagent, DSS (1 mg mL^{-1}, 10 mL) for 1 h. The activated Ag@TiO_2 isolated by centrifugation, and rinsed thrice with Mili-Q water. Van (0.1 mg mL^{-1}, 10 mL) was added and mixed with activated Ag@TiO_2 for 2 h. The functionalised nanoparticles were separated by centrifugation and washed with Mili-Q water to remove unbound Van. Finally, Van-functionalised nanoparticles were obtained.

2.3. Photocatalytic degradation of methylene blue

MB was selected as a model chemical to examine whether Van-Ag@TiO_2 nanoparticles possess photocatalytic activity after the surface immobilised with Van. In a typical experiment, MB solution (50 mL, 10 mg L^{-1}) and 10 mg of catalyst were placed in a culture tube. The suspension was stirred in the dark for 60 min before irradiation to reach an adsorption/desorption equilibrium between MB and the surface of the catalyst under room temperature. The photocatalytic reaction was started by irradiation of the mixture with UV. A 300 W UV lamp (Clipley Electrical Industrial Co., Ltd, China) with emission between 320 and 390 nm (broad maximum at 355 nm) was placed over the cube as the light source. The reaction temperature was maintained at 25 °C.

2.4. Antimicrobial and bactericidal assays

The antimicrobial activities of catalysts absorbed within the bacteria (Scheme 2) were assessed using the most probable number method (MPN), according to the American Society of Testing materials standard D4412-84, to determine variations in microbial populations of Van-sensitive bacteria, SRB. After the pure SRB culture was grown in modified Postgate's medium containing 2 g magnesium sulphate, 1 g ammonium chloride, 0.5 g sodium sulphate, 0.1 g calcium chloride, 0.5 g dipotassium hydrogen phosphate, 2 mL sodium lactate, and 7.5 g yeast extract/L at 30 °C for 4 d, bacterial cells were then isolated through centrifugation (6000 rpm, 20 min) and rinsed thrice with sterilised water. The culture tubes were irradiated using UV light in aqueous dispersions (50 mL) containing 25 mg of Ag, Ag@SiO_2, Ag@TiO_2, and Van-Ag@TiO_2 nanoparticles. To ensure complete mixing, the nanoparticles/bacterial mixture was magnetically stirred (100 rpm s^{-1}) under UV irradiation. At given irradiation time intervals, 5 mL bacterial suspensions were collected and counted via MPN method to assess the bactericidal activity of different nanomaterials. The MPN method, otherwise known as the method of Poisson zeroes, is a method of getting quantitative data on concentrations of discrete items from positive data. To increase the statistical accuracy of this test, the standard MPN procedure used a minimum of five tubes per dilution. After incubation for 15 d, the pattern of the positive tubes was noted, and a standardized MPN table was consulted to determine the most probable number of microorganisms per unit volume of the original sample. The Van-

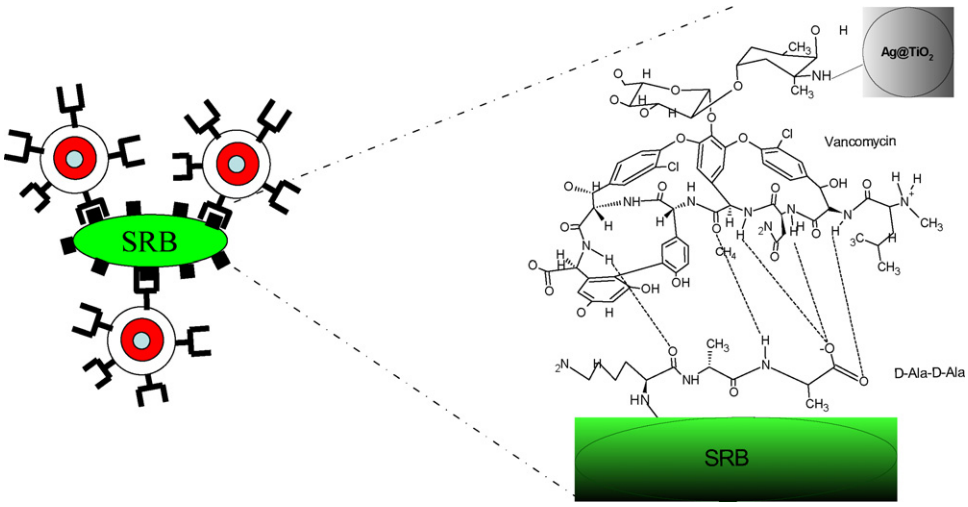

Scheme 2. Illustration of a multivalent interaction between Van-Ag@TiO_2 nanoparticles and SRB.

resistant bacteria, *V. anguillarum*, was used as the negative control to examine the bactericidal activity of Van-Ag@TiO_2 nanoparticles.

2.5. Characterisation of samples

Bacterial cells (1.7×10^7 cfu/mL) were mixed with 0.2 mg mL^{-1} of Van-Ag@TiO_2 nanoparticles, and the suspension was irradiated under UV light. The complex formed by bacterial cells and functionalised nanoparticles was centrifuged and harvested. TEM images (JEOL 2000FX, Japan) and UV–Vis absorption spectra (model 757CRT) were obtained. Powder XRD of the catalyst was recorded on a D8 Advance X diffractometer (Bruker Axs GmbH, Karsruhe, Germany) with a Cu Kα radiation. FT-IR spectroscopy (Nicolet iS10, Thermo electron scientific instruments LLC) was used to elucidate Van modification on the surface of Ag@TiO_2 nanoparticles.

3. Results and discussion

3.1. Synthesis and characterisation of catalyst

Nanocomposites were prepared in a simple and facile method through the hydrolysis of TEOS and titanium isopropoxide in the presence of Ag particles. The thickness of the shell can be readily tuned by controlling the amount of TEOS and titanium and the reaction time [19]. The TEM images of the synthesised core–shell nanoparticles are illustrated in Fig. 1. As shown, the shell layer containing TiO_2 and SiO_2 was uniformly coated on the core particle surface. The images also illustrated that the core–shell nanoparticles were monodispersed and spherical in shape. The diameter of the core and the thickness of the shell layer were ca. 90 and 20 nm, respectively.

The XRD pattern of the core–shell nanoparticles is shown in Fig. 2. Characteristic peaks were observed at 2θ values of 38.16°, 44.34° and 64.48°, corresponding to (1 1 1), (2 2 0), and (2 2 0) planes of Ag, and at $2\theta = 27.84°$, 36.50° and 42.84°, corresponding to the diffraction peaks of rutile TiO_2. Furthermore, Ag_2O may be doped into the Ag particle in the synthesis of core–shell nanoparticles. Unfortunately, only one peak appeared at $2\theta = 32.24°$ for the (1 1 1) plane of Ag_2O (Fig. 2). This is because the diffraction peaks of Ag were strong and the amount of the Ag_2O was low. The other intense peak corresponding to Ag_2O was covered by peaks corresponding to the Ag composite. Kuo et al. [20] reported that $2\theta = 32.24°$ can be assigned to Ag_2O (1 1 1) in the analysis of Ag particles incorporated on TiO_2 coating for the photodecomposition of *o*-cresol. Furthermore, the intensity of the characteristic diffraction peaks of TiO_2 was weak because the TiO_2 composite content was far

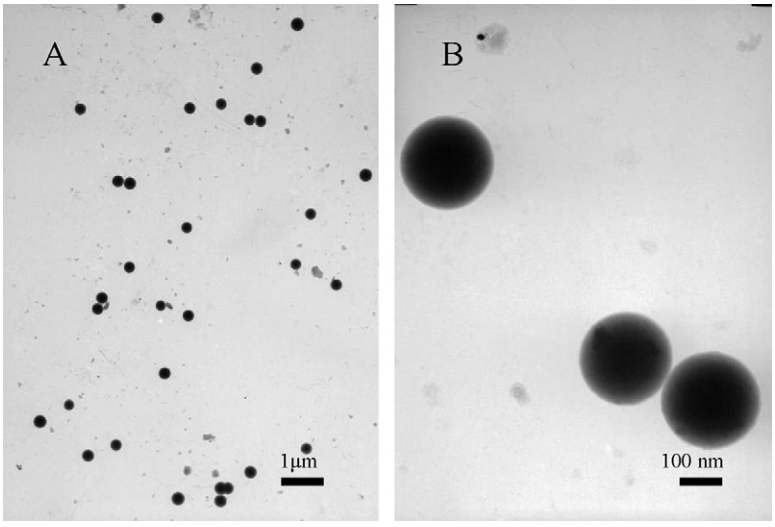

Fig. 1. TEM images of Van-Ag@TiO_2 with a ratio of 5000× (A) and 50,000× (B).

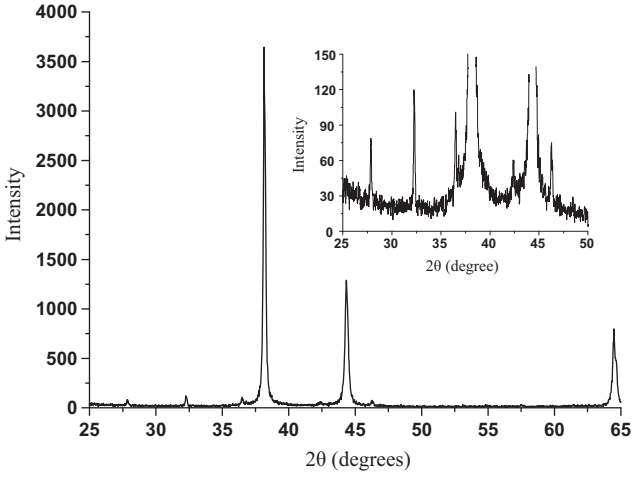

Fig. 2. XRD pattern of Van-Ag@TiO_2 nanoparticles. The inset is the enlarged version of this figure.

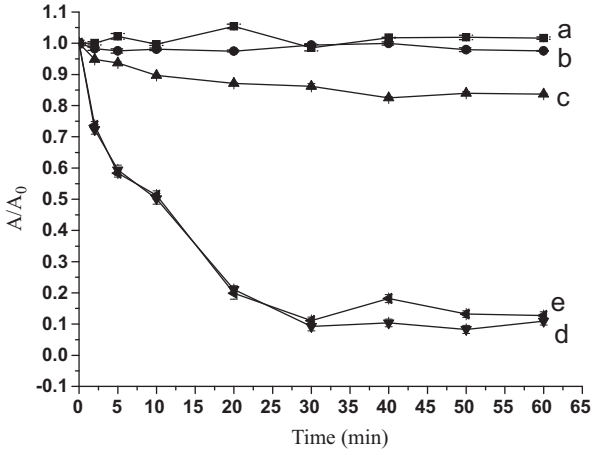

Fig. 4. Relative absorbance at 665 nm in the adsorption spectra of MB (10 mg L^{-1}, 50 mL) in aqueous dispersions containing MB in solution (a) and 10 mg catalysts under UV light irradiation: Ag (b), Ag@SiO_2 (c), Ag@TiO_2 (d), and Van-Ag@TiO_2 (e).

less than that of the Ag composite. Furthermore, the characteristic diffraction peaks of silica were not observed in the sample, which indicated that silica had an amorphous phase. This was because hydrosol restricted the crystallinity of the aforementioned composition. Based on the XRD and TEM results, TiO_2 and SiO_2 were coated uniformly on all the walls of the Ag nanoparticle core.

The FT-IR spectra (Fig. 3) of vancomycin, Ag@TiO_2, and Van-Ag@TiO_2 nanoparticles were measured. Based on the published research [21], the peaks [Fig. 3(b) and (c)] at 900–1100 cm^{-1} corresponded to the stretching vibration of Si–O–Si and the vibration of Si–O–Ti, and peaks at 785 and 461 cm^{-1} were attributed to the symmetric and deformation stretching of the Si–O–Si bond. Bands at 3500 and 1620 cm^{-1} represented the stretching and bending vibrations of the O–H bond. Compared to the FT-IR spectra of Ag@TiO_2, three new bands were observed for Van-Ag@TiO_2 at 1520, 1390, and 1330 cm^{-1}, which were attributed to aromatic adsorption. This implied that the surface of the Ag@TiO_2 nanoparticle was modified by Van.

The number of vancomycin molecules bound to the surfaces of the Ag@TiO_2 nanoparticles was estimated using UV–visible absorption spectroscopy [22]. We obtained that 1.1×10^{-9} mol (equivalent to 1.5 μg) of vancomycin was immobilized onto the surface of 1 mg of catalyst based on the relative absorption at a wavelength of 280 nm between a solution of Van (1.0 mg mL^{-1}) and the supernatant solution containing Van-Ag@TiO_2 nanoparticle (1 mg mL^{-1}). We estimated that there are 3.5×10^6 Van molecule immobilized on the surface of nanoparticles.

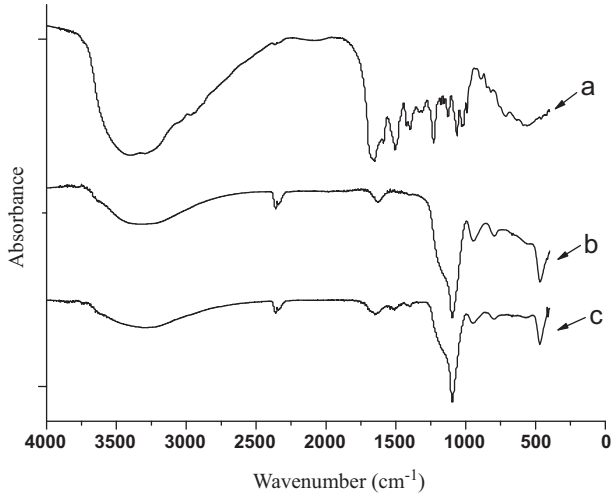

Fig. 3. FT-IR absorption spectra of vancomycin (a), Ag@TiO_2 (b), and Van-Ag@TiO_2 (c).

3.2. Photocatalytic degradation of methylene blue

Fig. 4 shows the UV irradiation time dependence of the relative absorbance (A/A_0) at the adsorption maximum wavelength of 665 nm for MB under different catalysts. Ag@TiO_2 and Van-Ag@TiO_2 exhibited a high level of MB degradation, such that the dye was degraded completely after 1 h under UV light irradiation. The photocatalytic degradation of MB generally followed a Langmuir–Hinshelwood mechanism, which could be simplified as a pseudo first order reaction [23]. However, a similar phenomenon did not occur in the degradation of MB over Ag and Ag@SiO_2 nanoparticles. Thus, the photocatalytic activities of the Ag@TiO_2 and Van-Ag@TiO_2 catalysts were similar. This means that Ag@TiO_2 nanoparticles still possessed photocatalytic activity after the surfaces immobilised with Van.

3.3. Bacterial inactivation under UV light irradiation and dark

The photocatalytic ability of Ag, Ag@SiO_2, Ag@TiO_2, and Van-Ag @TiO_2 for the destruction of SRB was assessed using 1.7×10^7 cfu/mL bacterial cell concentration. The photocatalytic reaction was started by the irradiation of a mixture containing catalysts and bacterial cells under UV light for 0–60 min. As shown in Fig. 5, the survival ratio in Ag and Ag@SiO_2 remains >90% as the illumination time is extended to 60 min. The SRB inactivation occurred using Ag@TiO_2 for 1 h of irradiation is two or three orders of magnitude higher than that using Ag and Ag@SiO_2 nanomaterials. The UV light itself and the photocatalysis did not significantly affect the degradation of bacteria in a short time (<1 h). However, SRB was almost completely killed within 1 h using Van-Ag@TiO_2 under UV light irradiation. The results indicated that the bacterial cell growth targeted by Van-Ag@TiO_2 was effectively inhibited and destroyed in the presence of the catalyst under UV light irradiation.

The Ag@TiO_2 showed a bactericidal effect for SRB under UV light irradiation. This was because $OH^{\bullet}$, $O_2^{\bullet -}$, and H_2O_2, which were generated by TiO_2 under UV irradiation, were responsible for bacterial inactivation. However, the photokilling mechanism remains unknown. Previously, researchers assumed that K^+ immediately leaked out and promptly increased bacterial inactivation. This is because K^+ plays a major role in the regulation of polysaccharide

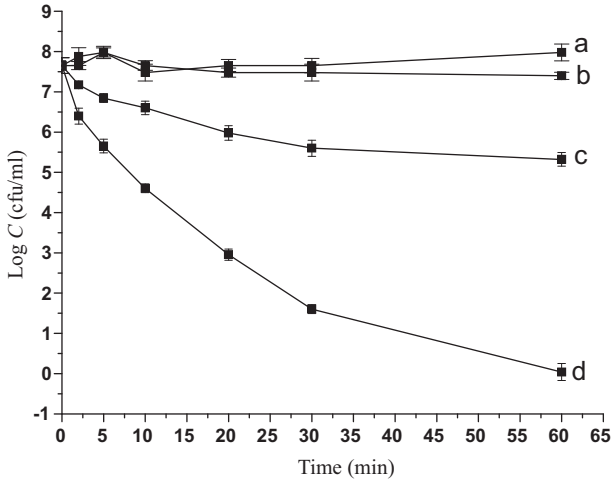

Fig. 5. Survival curve for SRB as a function of the UV light-irradiation in aqueous dispersions (50 mL) containing 25 mg of Ag (a), Ag@SiO_2 (b), Ag@TiO_2 (c), and Van-Ag@TiO_2 (d) nanoparticles.

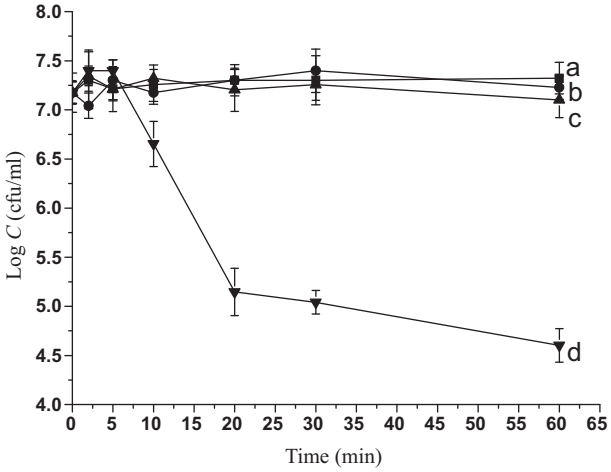

Fig. 7. Temporal course of SRB survival curve in aqueous dispersions (50 mL) containing 25 mg of Ag (a), Ag@SiO_2 (b), Ag@TiO_2 (c), and Van-Ag@TiO_2 (d) nanoparticles in the dark.

content and protein synthesis [11]. Other researchers proposed that the direct photocatalytic oxidation of coenzyme A was the primary cause of bacterial inactivation [24]. In addition, the pre-oxidation of the membrane phospholipids promoted by the TiO_2 photocatalyst was also suggested as a significant mechanism for bacterial inactivation [25].

However, the photocatalytic activity of Ag@TiO_2 for the destruction of SRB was far less than that of Van-Ag@TiO_2. This could be ascribed to two factors. An amount of Van-Ag@TiO_2 nanoparticles could be bound onto the surface of the bacterial cell based on the receptor–ligand recognition between Van and the D-Ala-D-Ala moiety. Naturally, the concentration of oxidizing radicals species that are close or proximal to cell wall in Van-Ag@TiO_2 was much higher than that in Ag@TiO_2, which may damaged all macromolecules (DNA, lipids and proteins) [26]. In addition, the multilayered effects of antibiotic–target bacteria interactions, including the essential cellular processes that are inhibited by bactericidal antibiotics and the associated cellular response mechanisms that contribute to killing [27]. Therefore, Van-Ag@TiO_2 exhibited a higher activity for SRB degradation under UV light. On the other hand, SRB can tolerate the low concentration of $OH^•$, $O_2^{•-}$, and H_2O_2 in Ag@TiO_2. SRB uses several strategies to deal with exposure to $OH^•$, $O_2^{•-}$ and H_2O_2. According to published report [28,29], these strategies could be divided into behavioural and molecular mechanisms. The former includes aggregate formation and aerotaxis, by which SRB is able to protect itself from full oxygen exposure by forming co-cultures or aggregates. The latter includes mechanisms, such as oxygen reduction and reactive oxygen species detoxification, which allow SRB to scavenge $OH^•$, $O_2^{•-}$, and H_2O_2 and prevent detrimental effects. The superoxide dismutase (SOD) enzyme neutralises most $OH^•$ radicals, and catalase eliminates the photogenerated H_2O_2.

Fig. 6 shows the TEM images of SRB in UV-illuminated Van-Ag@TiO_2 suspensions. As a result of TEM investigation (Fig. 6B), the outer membrane of the cell was not damaged, and few catalyst nanoparticles adhered to the outer membrane of the cell. This was because SRB tolerates a low concentration of $OH^•$, $O_2^{•-}$, and H_2O_2. When a certain amount of catalysts were bound to the surface of the cell wall, a greater destruction and degradation of the cell membrane was observed (Fig. 6C).

The inactivation of SRB was also evaluated in the dark in the presence of Van-Ag@TiO_2. In the same condition, Ag, Ag@SiO_2, and Ag@TiO_2 did not show any bactericidal effects on SRB (Fig. 7). This indicated that the phototoxicity to SRB was not from the photocatalyst itself but from oxidative stress produced by UV irradiation. However, The SRB inactivation occurred using Van-Ag@TiO_2 for 1 h in dark is two or three orders of magnitude higher than that using other nanomaterials. This was because the Van modified on the surface of nanoparticles is capable of enhancing the bactericidal effects in short time due to the antibotic–target interaction. Without sufficient cross-linking, the cell wall became mechanically fragile and the bacteria lysed. Hence, the bacteria could not grow from aqueous media. Compared with the study of MB degradation (Fig. 4), there is virtually no difference between Ag@TiO_2 and Van-

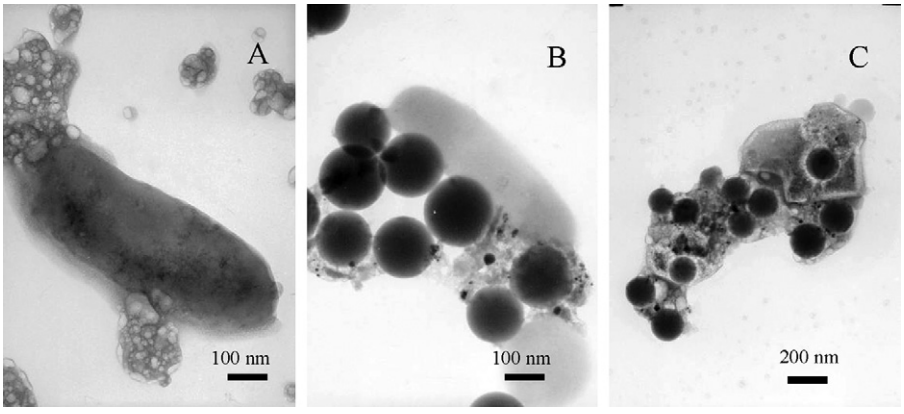

Fig. 6. TEM images of SRB in UV light-illuminated Van-Ag@TiO_2 suspensions (25 mg catalyst/50 mL): SRB before reaction (a), SRB treated for 30 min (b) and 60 min (c).

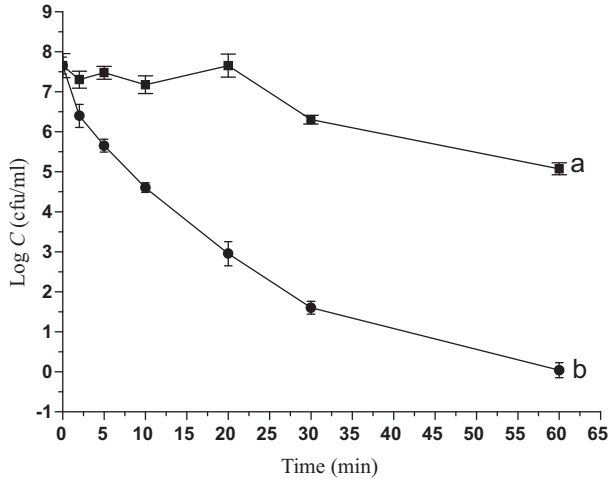

Fig. 8. Temporal course of *Vibrio anguillarum* (a) and SRB (b) survival curve in aqueous dispersions (50 mL) containing 25 mg Van-Ag@TiO_2 in UV light irradiation.

Ag@TiO_2 for degradation of MB. However, there is a large difference between Ag@TiO_2 and Van-Ag@TiO_2 for bactericidal properties of SRB. The difference of results due that the D-Ala-D-Ala structure on the surface of cell wall can be recognized with vancomycin.

3.4. Specificity of phototoxicity to Van-sensitive bacteria

Fig. 8 further verified that Van-Ag@TiO_2 showed a limiting selective phototoxicity for the Van-sensitive bacteria, SRB. It was almost completely killed within 1 h in Van-Ag@TiO_2 under UV light irradiation. The partial inactivation of Van-insistent bacteria, *V. anguillarum*, occurred under the same condition. These results indicated that Van-Ag@TiO_2 was capable of selective phototoxicity to the Van-sensitive bacteria, SRB. Functionalised molecules modified onto the surface of the nanoparticle to enhance antimicrobial activities have recently gained academic interest. In addition, the SRB inactivation occurred using Van-Ag@TiO_2 for 1 h of irradiation is four orders of magnitude higher than that for 1 h in dark, which is due to antibacterial function of TiO_2 under UV light irradiation.

Au@Van nanoparticles exhibited enhanced activities against Van-resistant enterococci and Gram-positive bacteria [15]. Furthermore, TEM indicated that the targeting capability of Van-Ag@TiO_2 for SRB was due to the five-point hydrogen bond formed between the bacteria and the nanoparticles. However, there were no nanoparticles on the membrane of Van-insistent bacteria, *V. anguillarum*, because Van-insistent bacteria have additional outer membranes that cover much of the cell surface. This membrane was highly impenetrable to vancomycin, restricting access to the D-Ala-D-Ala moiety [18]. As a result, the functionalised Ag@TiO_2 nanoparticles were hardly bound onto the cell wall of *V. anguillarum*.

4. Conclusions

Van-Ag@TiO_2 showed high UV light-driven bactericidal activity for Gram-positive bacteria, SRB. The functionalised catalysts were fabricated based on the unique features of TiO_2, such as its photocatalytic activity and ability to self-assemble dopamine into the surface. The improvement of bactericidal activity under UV irradiation is due to the targeting capacity of Van-functionalised nanoparticles for the bacteria. This photocatalyst can be used to inhibit and destroy other bacteria for food safety control and environmental contamination. The bactericidal efficiency and killing mechanisms of catalysts under UV light were illustrated and discussed. The nanoparticle composite showed excellent potential applications for selective photokilling of pathogenic bacteria. The role of the Ag core in the catalyst will be further investigated.

Acknowledgments

The author would like to thank Dr. Zhaolan Mo for the contribution of *V. anguillarum*. This work was supported by the National Natural Science Foundation of China (Grant No. 41076047), Chinese Academy of Sciences (Grant KZCX2-YW-205-03) and Shandong Provincial Natural Science Foundation, China (Grant No. ZR2010DM004).

References

[1] M. Anpo, S. Dohshi, M. Kitano, Y. Hu, M. Takeuchi, M. Matsuoka, The preparation and characterization of highly efficient titanium oxide-based photofunctional materials, Annu. Rev. Mater. Res. 35 (2005) 1–27.
[2] A.-N. Chowdhury, M.S. Azam, M. Aktaruzzaman, A. Rahim, Oxidative and antibacterial activity of Mn_3O_4, J. Hazard. Mater. 172 (2009) 1229–1235.
[3] C.E. Lawrence, P.R. Taylor, B.J. Trock, A.A. Reilly, Trihalomethanes in drinking-water and human colorectal-cancer, J. Natl. Cancer Inst. 72 (1984) 563–568.
[4] P.S.M. Dunlop, J.A. Byrne, N. Manga, B.R. Eggins, The photocatalytic removal of bacterial pollutants from drinking water, Photochem. Photobiol. A: Chem. 148 (2002) 355–363.
[5] F. Sayllkan, M. Asiltük, N. Kiraz, E. Burunkaya, E. Arpa, H. Sayllkan, Photocatalytic antibacterial performance of Sn^{4+}-doped TiO_2 thin films on glass substrate, J. Hazard. Mater. 162 (2009) 1309–1316.
[6] C.A. Linkous, G.J. Carter, D.B. Locuson, A.J. Ouellette, D.K. Slattery, L.A. Smitha, Photocatalytic inhibition of algae growth using TiO_2, WO_3, and cocatalyst modifications, Environ. Sci. Technol. 34 (2000) 4754–4758.
[7] W. Su, S.S. Wei, S.Q. Hu, J.X. Tang, Preparation of TiO_2/Ag colloids with ultraviolet resistance and antibacterial property using short chain polyethylene glycol, J. Hazard. Mater. 172 (2009) 716–720.
[8] D.M. Blake, P.C. Maness, Z. Huang, E.J. Wolfrum, J. Huang, W.A. Jacoby, Application of the photocatalytic chemistry of titanium dioxide to disinfection and the killing of cancer cells, Sep. Purif. Rev. 28 (1999) 1–50.
[9] L. Zhang, J.C. Yu, H.Y. Yip, Q. Li, K.W. Kwong, A.-W. Xu, P.K. Wong, Ambient light reduction strategy to synthesize silver nanoparticles and silver-coated TiO_2 with enhanced photocatalytic and bactericidal activities, Langmuir 19 (2003) 10372–10380.
[10] Y. Lan, C. Hu, X. Hu, J. Qu, Efficient destruction of pathogenic bacteria with AgBr/TiO_2 under visible light irradiation, Appl. Catal. B 73 (2007) 354–360.
[11] C. Hu, Y. Lan, J. Qu, X. Hu, A. Wang, Ag/AgBr/TiO_2 visible light photocatalyst for destruction of azodyes and bacteria, J. Phys. Chem. B 110 (2006) 4066–4072.
[12] M.R. Elahifard, S. Rahimnejad, S. Haghighi, M.R. Gholami, Apatite-coated Ag/AgBr/TiO_2 visible-light photocatalyst for destruction of bacteria, J. Am. Chem. Soc. 129 (2007) 9552–9553.
[13] P. Wu, R. Xie, J.A. Imlay, J.K. Shang, Visible-light-induced photocatalytic inactivation of bacteria by composite photocatalysts of palladium oxide and nitrogen-doped titanium oxide, Appl. Catal. B 88 (2009) 576–581.
[14] J.A. Rengifo-Herrera, E. Mielczarski, J. Mielczarski, N.C. Castillo, J. Kiwi, C. Pulgarin, *Escherichia coli* inactivation by N, S co-doped commercial TiO_2 powders under UV and visible light, Appl. Catal. B 84 (2008) 448–456.
[15] H. Gu, P.L. Ho, E. Tong, L. Wang, B. Xu, Presenting vancomycin on nanoparticles to enhance antimicrobial activities, Nano Lett. 3 (2003) 1261–1263.
[16] C. Walsh, Microbiology: deconstructing vancomycin, Science 284 (1999) 442–443.
[17] H. Gu, P.-L. Ho, K.W.T. Tsang, L. Wang, B. Xu, Using biofunctional magnetic nanoparticles to capture vancomycin-resistant enterococci and other gram-positive bacteria at ultralow concentration, J. Am. Chem. Soc. 125 (2003) 15702–15703.
[18] A.J. Kell, G. Stewart, S. Ryan, R. Peytavi, M. Boissinot, A. Huletsky, M.G. Bergeron, B. Simard, Vancomycin-modified nanoparticles for efficient targeting and preconcentration of gram-positive and gram-negative bacteria, ACS Nano 2 (2008) 1777–1788.
[19] A. Guerrero-Martinez, J. Perez-Juste, L.M. Liz-Marzan, Recent progress on silica coating of nanoparticles and related nanomaterials, Adv. Mater. 22 (2010) 1182–1195.
[20] Y.-L. Kuo, H.-W. Chen, Y. Ku, Analysis of silver particles incorporated on TiO_2 coatings for the photodecomposition of o-cresol, Thin Solid Films 515 (2007) 3461–3468.
[21] P. Novotn, J. Zita, J. Krýsa, V. Kalousek, J. Rathousk, Two-component transparent TiO_2/SiO_2 and TiO_2/PDMS films as efficient photocatalysts for environmental cleaning, Appl. Catal. B 79 (2008) 179–185.
[22] Y.-S. Lin, P.-J. Tsai, M.-F. Weng, Y.-C. Chen, Affinity capture using vancomycin-bound magnetic nanoparticles for the MALDI-MS analysis of bacteria, Anal. Chem. 77 (2005) 1753–1760.

[23] R. Nakamura, A. Imanishi, K. Murakoshi, Y. Nakato, In situ FTIR studies of primary intermediates of photocatalytic reactions on nanocrystalline TiO_2 films in contact with aqueous solutions, J. Am. Chem. Soc. 125 (2003) 7443–7450.
[24] T. Matsunaga, R. Tomoda, T. Nakajima, N. Nakamura, T. Komine, Continuous-sterilization system that uses photosemiconductor powders, Appl. Environ. Microbiol. 54 (1988) 1330–1333.
[25] P.C. Maness, S. Smolinski, D.M. Blake, Z. Huang, E.J. Wolfrum, W.A. Jacoby, Bactericidal activity of photocatalytic TiO_2 reaction: toward an understanding of its killing mechanism, Appl. Environ. Microbiol. 65 (1999) 4094–4098.
[26] E. Cabiscol, J. Tamarit, J. Ros, Oxidative stress in bacteria and protein damage by reactive oxygen species, Int. Microbiol. 3 (2000) 3–8.
[27] M.A. Kohanski, D.J. Dwyer, J.J. Collins, How antibiotics kill bacteria: from targets to networks, Nat. Rev. Microbiol. 8 (2010) 423–435.
[28] H. Cypionka, Oxygen respiration by desulfovibrio species, Annu. Rev. Microbiol. 54 (2003) 827–848.
[29] D.J. Hassett, M.S. Cohen, Bacterial adaptation to oxidative stress: implications for pathogenesis and interaction with phagocytic cells, FASEB J. 3 (1989) 2574–2582.